PERFORMANCE OF SERIES CIRCUIT CONFIGURATION ON PIEZOELECTRIC SENSORS COATED WITH Zn-DOPED CARBON DOTS AS ENERGY GENERATING SPEEDBUMPS

Fauziyah Vida Rahmah Wijaya, Akbar Sujiwa, Nur Aini Fauziyah*

Department of Physics, Faculty of Engineering and Science, Universitas Pembangunan Nasional "Veteran" Jawa Timur, Indonesia

Received: 13th December 2025; Revised: 13rd February 2026; Accepted: 2nd April 2026

ABSTRACT

The increasing demand for electrical energy has driven the exploration of alternative energy sources. The mechanical energy generated by vehicles passing over speed bumps can be harvested on a small scale using piezoelectric sensors. This study investigates the performance enhancement of piezoelectric elements coated with Zn-doped Carbon Dots (CDs) and their application in a series-configured energy-harvesting speedbump. Zn-doped CDs were synthesized using the sol-gel method, and the materials were characterized by XRD, SEM, EDX, and mechanical testing of the piezoelectric sensors under varying loads. XRD characterization indicates that the commercial piezoelectric material contains $BaTiO_3$ as the primary phase and BaO as the secondary phase. SEM EDX analysis confirms that the particle size distribution of Zn-doped CDs ranges from 0 to 2400 nm. Single-element testing of the PLRCZ layer shows that the piezoelectric sensor with a resin/Zn-doped CDs coating generates a higher voltage compared to the uncoated sensor under a load of 122.8 g. In the series configuration, the output voltage decreases at each load point, reaching a maximum of 1 V, while across all PLRCZ elements, the voltage reaches a maximum of 0.4 V, with no detectable current.

Keywords: piezoelectric sensor; speedbump; Zn-doped CDs

Introduction

Global energy demand continues to rise significantly due to population growth and increasing industrial activity.[1] The extensive reliance on fossil-fuels, such as coal and petroleum, must be reduced to mitigate environmental degradation and climate change.[2] Consequently, the development of alternative energy sources, including solar, wind[3], and mechanical energy,[4] has become a strategic approach to addressing the global energy crisis. While renewable energy implementation is often associated with large-scale systems such as solar and wind power plants, small-scale energy-harvesting technologies also offer considerable potential. One such approach involves utilizing the increasing number of motor vehicles on highways as a source of mechanical energy. The mechanical energy dissipated by vehicles during motion and deceleration can be harvested and converted into electrical energy using energy-harvesting speed bumps.[5] The development of small-scale power generation technologies based on piezoelectric sensors integrated into speed bumps can contribute to achieving the seventh Sustainable Development Goals (SDGs) on clean and affordable energy, as well as the eighth SDGs through technological innovation that adds economic value and promotes sustainable economic productivity. In Indonesia, the widespread deployment of speed bumps presents significant opportunities for mechanical energy harvesting. Each vehicle passing over a speed bump generates mechanical pressure from rapid deceleration, which can be converted into electrical energy using piezoelectric sensors. In high-traffic locations, a single speed bump may be traversed by thousands of vehicles daily, offering substantial potential for electricity generation.

*Corresponding author.
E-Mail: nur.aini.fisika@upnjatim.ac.id

Piezoelectric sensors have emerged as a promising alternative for electrical energy generation. In general, piezoelectric materials act as transducers capable of converting mechanical deformation into electrical energy, and vice versa, in accordance with the principle of piezoelectric duality.[6] Owing to their affordability, ease of fabrication, and high efficiency in converting mechanical signals into electrical signals,[7] Piezoelectric materials have been widely adopted in structural health monitoring applications. Piezoelectric energy harvesting technology enables the capture and utilization of ambient vibrational energy commonly present in human environments, including mechanical equipment, buildings, highways, and railway systems. In transportation applications, piezoelectric sensors can be engineered to harvest mechanical energy dissipated by vehicle loads, which can then be stored in rechargeable energy storage devices. The harvested energy may be utilized to power traffic lights, electronic signage, lighting systems, and roadside safety infrastructure.[8] The electrical voltage generated by a piezoelectric sensor can reach several volts, depending on the material properties, sensor dimensions, and applied mechanical pressure. Furthermore, the harvested electrical energy can be stored in various energy storage systems, such as rechargeable batteries, enabling practical and sustainable energy utilization.

Empty Fruit Bunches (EFB) from oil palm possess material characteristics that enable their conversion into carbon-based materials, with cellulose content of 36.81%, hemicellulose content of 27.01%, and lignin content of 15.07%. Lignin isolated from EFB shows significant potential as a precursor for the synthesis of carbon-based nanomaterials, particularly carbon dots (CDs).[9] CDs synthesized from EFB have been reported to enhance electrical conductivity and energy storage capacity.[10] Naturally derived CDs exhibit excellent fluorescence properties, nanoscale dimensions, and high biocompatibility, which can be further improved through heteroatom doping, such as nitrogen, sulfur, or phosphorus, or via surface passivation.[11] The dual capability of CDs to serve as both electron donors and acceptors enables chemiluminescence and electrochemiluminescence, making them highly attractive for applications in catalysis, optoelectronics, and sensing systems.[12] Recently, metal-doped CDs, particularly Zn-doped CDs, have garnered increasing attention due to their enhanced functional properties. Metal doping significantly alters the physicochemical properties of CDs, leading to improved fluorescence intensity, tunable energy band gaps, increased electrical conductivity, and enhanced photocatalytic performance. Moreover, doped CDs exhibit superior electron-transfer and electron-accepting properties, making them suitable for advanced electronics and energy-storage applications.[13]

Numerous previous studies have demonstrated the potential of piezoelectric sensors for energy harvesting applications. Sidiq,[14] designed a speedbump prototype incorporating 38 piezoelectric sensors that utilized vehicle-induced pressure to generate electrical energy, achieving a maximum output voltage of 17.88 V and an average power of 2.9 W. In a more specific application, Apriyanto,[15] reported that a 35 mm diameter piezoelectric sensor installed on a staircase was capable of harvesting energy for a wireless sensor network, producing a maximum energy output of 297.4 µJ using eight sensor elements. However, increasing the number of elements did not necessarily result in a proportional increase in harvested energy due to non-uniform pressure distribution. Pradistia,[16] evaluated a piezoelectric staircase floor prototype with three electrical configurations and found that the configuration consisting of five parallel and four series connections yielded the highest voltage and current output during downhill motion. In the context of Carbon Dots (CDs), Dona,[17] synthesized CDs from natural precursors, specifically oil palm Empty Fruit Bunches (EFB). Nevertheless, existing studies have not yet investigated the application of Zn-doped CDs as a surface

coating to enhance the electrical output performance of a piezoelectric sensor.

Therefore, this research aims to develop a piezoelectric sensor for speed bump applications by employing Zn-doped CDs derived from oil palm EFB as a surface coating to enhance the electrical output performance of the piezoelectric sensor. In this study, the piezoelectric sensors were arranged in series for implementation in a speed bump system. The characterization procedures included X-Ray Diffraction (XRD) analysis of the piezoelectric material to identify its crystal phase, Scanning Electron Microscopy-Energy Dispersive X-ray Spectroscopy (SEM EDX) analysis of the Zn-doped CDs to evaluate particle size distribution, and mechanical testing under varying loads to assess the electrical output of the Zn-doped CDs-coated piezoelectric sensors in terms of voltage, current, and power.

Methods

This research commenced with the preparation of the required materials and equipment. The materials used for the piezoelectric sensor assembly included a wooden board, ten piezoelectric disk sensors with a diameter of 35 mm, KBJ308 bridge rectifier diodes, and the MT3608 step-up module. For the synthesis of Zn-doped CDs, the materials consisted of 0.8 g of carbonized oil palm EFB, prepared following the method reported by Dona[17], ZnO SAP (99% purity), HCl SAP 37%, and epoxy resin. The piezoelectric sensor employed in this study were commercially available device with a golden yellow appearance, a nominal capacitance of 30.0 pF ± 30%, and a maximum input voltage range of 1.5~30 Vp-p. The equipment utilized during the experimental procedures included a soldering iron, calibrated test weights (122.8 g, 1 kg, 2 kg, and 2,8 kg), a digital multimeter, and an oven.

Subsequently, the synthesized CDs were subjected to a doping process. Zn was incorporated into the CDs structure using the sol-gel method. In this procedure, a $ZnCl_2$ solution was prepared by reacting 0.3 M ZnO with 0.6 M HCl (10 mL), followed by the addition of 10 mL of CDs solution. The mixture was continuously stirred using a magnetic stirrer at 200°C for 1 h to facilitate the sol-gel reaction. Upon completion of the process, a precipitate was formed. The resulting homogeneous precipitate was then dried in an oven at 125°C for 25 minutes to obtain Zn-doped CDs powder. To evaluate the success of the doping process, the Zn-doped CDs powder was characterized using SEM-EDX (Zeiss, 5.00 kV, 6.3 mm × 20.0 K) to analyze the morphology and particle size of the Zn-doped CDs samples.

The subsequent step involved compositing the Zn-doped CDs powder with epoxy resin. The mixture was prepared by combining 15 mL of epoxy resin with 0.02 g of Zn-doped CDs, then mechanically stirring to achieve a homogeneous dispersion. The resulting epoxy resin/Zn-doped CDs composite was applied as a coating onto the surface of the piezoelectric sensor. The coated piezoelectric sensor elements were subsequently connected in series, as illustrated in Figure 1, and output measurements were taken at each element to evaluate the electrical response.

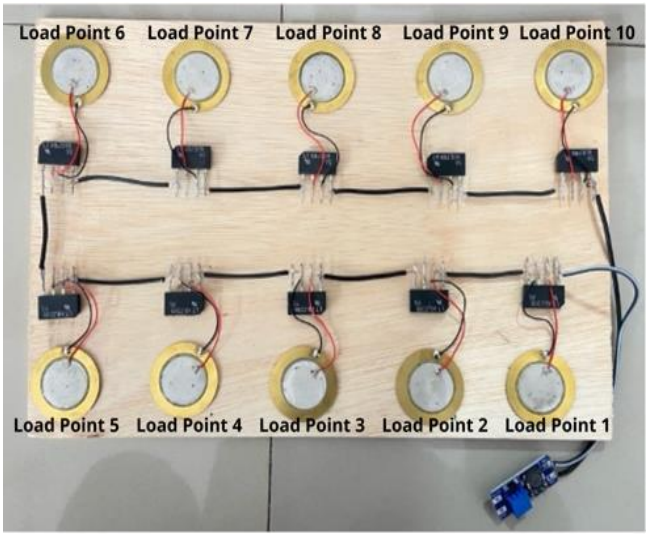

Figure 1. Configuration of the Series Circuit of Zn-Doped CDs Layered Piezoelectric Sensors

Before the series connection, the commercial piezoelectric material was

characterized using XRD (Philips) (2θ = 15-65, Cu-Kα) to determine the phase composition of the sample. As illustrated in Figure 1, the speedbump prototype design incorporates ten piezoelectric disk sensors with a diameter of 35 mm, each integrated with a KBJ308 bridge rectifier diode to convert alternating current (AC) into direct current (DC) and to regulate the electrical output of individual piezoelectric elements, thereby preventing mutual interface. The MT3608 step-up module was employed to stabilize and boost the fluctuating piezoelectric output voltage to a level suitable for charging applications. The sample nomenclature is shown in Table 1.

Table 1. Nomenclature of Piezoelectric Sensor Samples

Sample Name	Description
PTL	Uncoated Piezoelectric Sensor
PLRCZ	Piezoelectric Sensor with Resin Coating + Carbon Dots doped with Zn

Table 2. Results of Phase Composition of Piezoelectric Sample

Phase Composition	Phase Content (n%)
$BaTiO_3$	88
BaO	12

During implementation, the PTL and PLRCZ units were evaluated by applying mechanical loads of varying magnitudes, followed by measurements of the generated voltage and current using a digital multimeter, from which the electrical power output was calculated. For comparison, the PLRCZ elements were additionally configured in a series arrangement and subjected to the same mechanical loading conditions, with the resulting output voltage measured using a digital multimeter. This approach was employed to assess and compare the electrical output performance of the series-connected PLRCZ configuration with that of the individual piezoelectric sensor units.

Result and Discussion

a. X-Ray Diffraction Measurement Spectrum

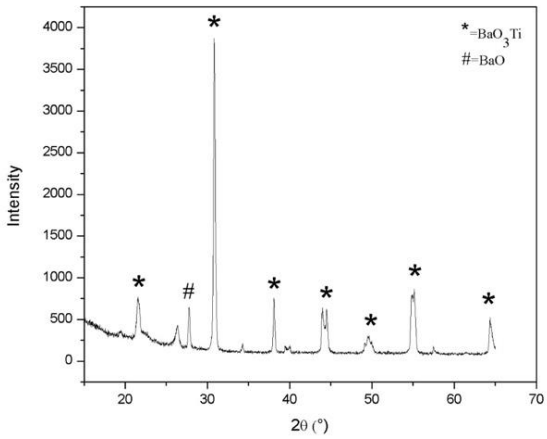

Figure 2. XRD Measurement Spectrum of Piezoelectric Sample

The XRD results of the piezoelectric material, presented in Figure 2, display characteristic diffraction peaks corresponding to different crystalline phases. Peaks marked with asterisks (*) are attributed to the $BaTiO_3$ (Barium Titanate) phase, while those indicated by hash symbols (#) correspond to the BaO (Barium Oxide) phase, confirming the presence of two distinct crystalline phases in the material. The most intense diffraction peak is observed at a 2θ angle of approximately 31°, which is characteristic of the $BaTiO_3$ phase. Additional diffraction peaks are distributed within the 2θ range of 20° to 65°, reflecting the overall crystalline structure of the material. Phase composition analysis, as summarized in Table 2, reveals that the piezoelectric material consists predominantly of $BaTiO_3$ with a dominant content of 88%, accompanied by a secondary BaO phase with a content of 12%. The dominance of the BaO_3Ti phase confirms the piezoelectric nature of the material, in agreement with COD No. 9016084. The presence of the BaO secondary phase, consistent with COD No. 5910030, indicates the existence of additional phase constituents within the piezoelectric sensor material.

$BaTiO_3$ material is widely used as a piezoelectric sensor material due to its ferroelectric nature and perovskite-type

crystal structure, which exhibits both piezoelectric and pyroelectric properties associated with nonlinear polarization reversal phenomena.[18] $BaTiO_3$ material can attain a dielectric constant of up to 7000, rendering it highly sensitive to variations in electric field and applied mechanical pressure.[19] The perovskite structure of $BaTiO_3$ enables the relative displacement of Ti^{4+} and O^{2-} ions with respect to Ba^{2+} ions, generating an electric dipole moment and spontaneous polarization.[18] This intrinsic dipole displacement allows the material to rapidly respond to changes in mechanical force through the piezoelectric effect.[20] In the present material system, a secondary BaO is also observed. Unlike $BaTiO_3$, BaO phase is not ferroelectric and exhibits significantly lower polarization. The polarization mismatch between the $BaTiO_3$ and BaO phases can induce internal electric fields and additional electrostatic energy, potentially leading to the formation of depolarization fields. However, in the piezoelectric samples studied, the $BaTiO_3$ phase is dominant, minimizing the depolarization field and keeping the material predominantly in a stable ferroelectric ground state.

b. SEM EDX

The SEM EDX characterization results of the Zn-doped CDs are presented in Figure 3. As shown in Figure 3a, the Zn-doped CDs exhibit nanoscale features with a coral-like morphology. The SEM image reveals a relatively uniform particle size distribution at a magnification of 20K, illustrating the surface morphology of the sample. Figure 3b presents the particle size distribution analysis performed using ImageJ software, where backscattered features are identified, with non-black regions representing individual particles and white regions indicating particles selected for analysis. Based on the particle size analysis shown in Figure 3c, processed using Origin software, the Zn-doped CDs display a particle size distribution within the nanometer scale. The most dominant carbon aggregates size range is 0-2400 nm, with the highest frequency reaching approximately 95 particles.

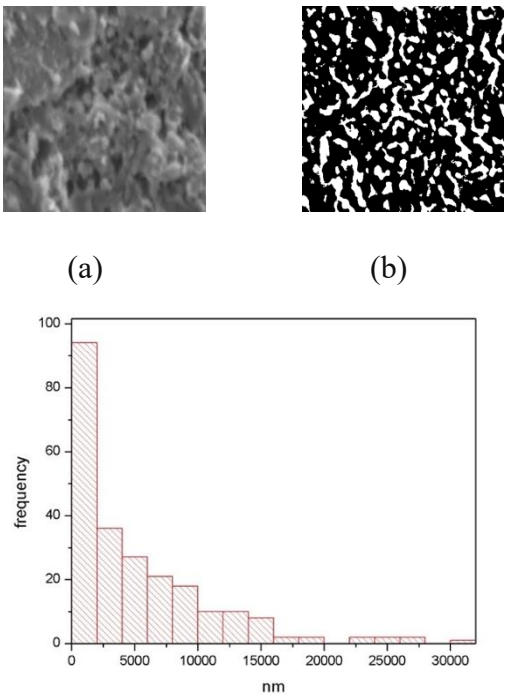

Figure 3. SEM EDX Test Results for Zn-doped CDs, (a) SEM Image at 20K Magnification, (b) Backscatter Image at 20K Magnification Analyzed Using ImageJ Software, (c) Carbon Aggregates Size Analysis of Sample from SEM Test Results Using Origin Software

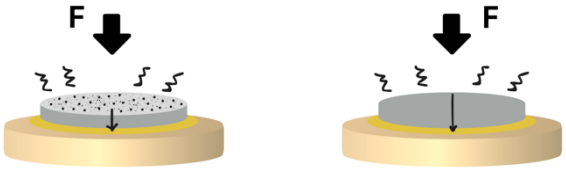

Figure 4. Piezoelectric Sensor, (a) With Zn-doped CDs Layer, (b) Without Layer

To enhance the conversion efficiency of mechanical energy into electrical energy in piezoelectric sensors, composite materials are required as surface coatings. The incorporation of composite layers aims to improve mechanical stress absorption and facilitate more effective transfer of applied pressure to the piezoelectric material, thereby enhancing energy conversion performance

Figure 4 schematically illustrates piezoelectric sensors without and with a Zn-doped CDs coating. As shown in Figure 4a, the piezoelectric sensor is coated with a Zn-

doped CDs layer. When mechanical pressure (F) the piezoelectric sensor is subjected to mechanical pressure (F) is applied, the Zn-doped CDs layer, composed of nanoscale particles, reinforces and stabilizes the structural arrangement of the sensor. Moreover, the uniformly distributed nano-sized CDs on the sensor surface act as a mediating layer that promotes more homogeneous pressure distribution across the piezoelectric material. In contrast, Figure 4b depicts an uncoated piezoelectric sensor. Under applied mechanical pressure (F), the load is directly transferred to the piezoelectric material, rendering the sensor more susceptible to damage under high loads due to the absence of a buffering layer capable of evenly distributing the applied stress. The contribution of CDs is also associated with their photoluminescent properties, which are significantly enhanced by Zn doping. Furthermore, the conductive nature of Zn facilitates more efficient charge transfer generated by the piezoelectric effect. This enhancement is closely related to the performance of the $BaTiO_3$ phase, as uniform pressure distribution enables optimal spontaneous polarization within the $BaTiO_3$ perovskite structure, resulting in more stable dipole moments.[18,20] Although the Zn-doped CDs layer is not electrically connected to the piezoelectric material, mechanical energy can still be efficiently absorbed and transferred to the piezoelectric sensor through interfacial energy transfer mechanisms. These findings are consistent with the piezoelectric sensor performance results summarized in Table 3, which compare sensors with and without Zn-doped CDs coatings.

Based on the data presented in Figure 5, the reported values represent the average of ten experimental trials, reflecting the direct current (DC) performance of single-element PTL and PLRCZ units. Under a load of 122.8 g, the PTL element generated a lower output voltage than the PLRCZ element. This behavior is attributed to the presence of the Zn-doped CDs coating, which enables more uniform distribution of mechanical stress under relatively light loads while simultaneously protecting the piezoelectric sensor surface (electrode) from mechanical deformation. When the applied load was increased to 1 kg, both sensors exhibited comparable average output voltages across ten measurements. At this load level, the PTL element experienced physical damage, including output cable breakage and surface abrasion caused by mechanical deformation under the relatively high load (Figure 6). Since damaged PTL elements could not be reused, they were replaced with new PTL elements in subsequent tests. This replacement introduced output variability and transient voltage spikes resulting from deformation of the remaining PTL elements. The presence of these transient spikes contributed to the comparable average output values observed for the PTL and PLRCZ elements during the 1 kg load test.

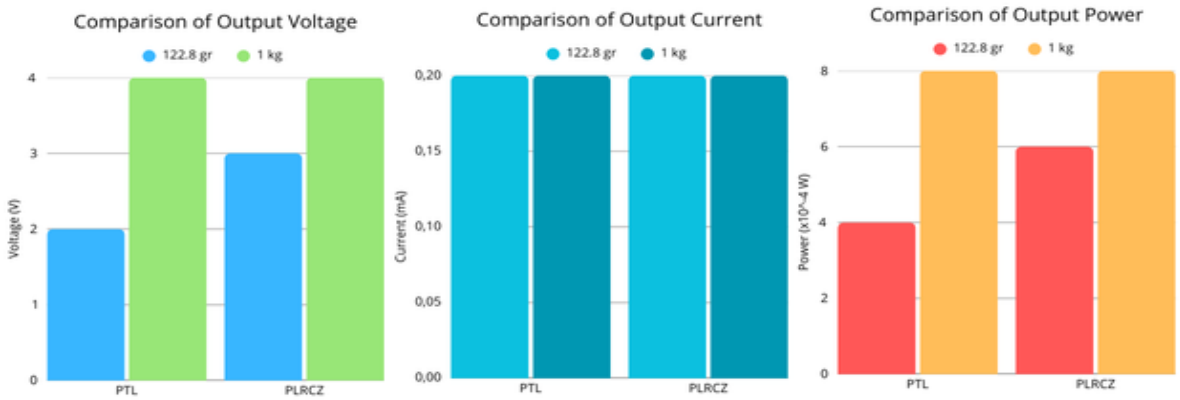

Figure 5. Results of Piezoelectric Sensor Testing for Direct Current (DC) Element Units, (a) Comparison of Output Voltage, (b)Comparison of Output Current, (c) Comparison of Output Power

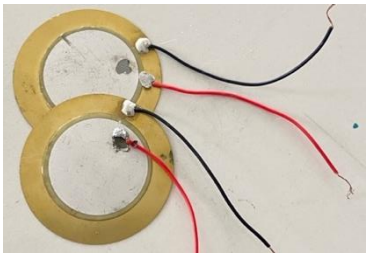

Figure 6. Damaged PTL Element

Table 3. Results of Testing the PLRCZ Series Circuit at Each Load Point

Series Circuit PLRCZ	Weight of The Load			
	1 kg		2 kg	
	Voltage (Volt)		Voltage (Volt)	
	1 Hz (5 seconds)	2 Hz (10 seconds)	1 Hz (5 seconds)	2 Hz (10 seconds)
Load Point 1	0,3 (1)	0,2 (5)	0,5 (5)	0,5 (4)
Load Point 2	0,2 (2)	0,4 (5)	0,3 (5)	0,2 (2)
Load Point 3	0,3 (2)	0,4 (4)	0,4 (2)	0,5 (7)
Load Point 4	0,4 (4)	0,4 (9)	0,4 (7)	0,7 (6)
Load Point 5	0,2 (2)	0,5 (3)	0,2 (4)	0,3 (4)
Load Point 6	0,3 (1)	0,7 (2)	0,5 (7)	0,8 (3)
Load Point 7	0,3 (4)	0,6 (2)	0,4 (5)	0,6 (4)
Load Point 8	0,2 (6)	0,4 (3)	0,4 (5)	0,5 (5)
Load Point 9	0,4 (2)	0,5 (8)	0,5 (5)	0,8 (2)
Load Point 10	0,6 (6)	0,6 (2)	0,6 (8)	1 (10)

The experimental results obtained from ten load points of the series-connected PLRCZ elements (Figure 1) reveal a substantial reduction in output voltage compared with the performance of individual PLRCZ elements reported in Figure 5. As summarized in Table 3, under a 1 kg load, the maximum voltage of 0.7 V (standard deviation of 0.2) was recorded at load point 6 at a tapping frequency of 2 Hz. For the 2 kg load condition, the highest output voltage of 1 V (standard deviation of 1.0) was observed at load point 10, also at a frequency of 2 Hz. The values in parentheses in Table 4 represent the standard deviation calculated from 10 test repetitions. In both loading conditions, the maximum voltages were observed at 2 Hz, corresponding to two load applications every 10 seconds (Figure 7). These results indicate that higher tapping frequencies yield higher average output voltages than lower frequencies (1 Hz). Overall, the series-connected PLRCZ elements subjected to a 2 kg load generated higher average output voltages than those tested under a 1 kg load, demonstrating that the applied load magnitude strongly influences the electrical output of the piezoelectric sensor. Greater mechanical

loads result in increased deformation of the piezoelectric material, thereby producing higher output voltages.

Figure 7. Testing the PLRCZ Series Circuit at Each Load Point

Table 4. Results of Testing the Series Circuit Configuration of Piezoelectric Sensors

Series Circuit PLRCZ	Weight of The Load	
	2,8 kg	
	Voltage (Volt)	
	1 Hz (5 second)	2 Hz (10 second)
All PLRCZ elements	0,2 (2)	0,4 (4)

Table 4 presents the output-voltage results from all PLRCZ elements connected in series. The measurements were conducted using a uniformly applied load of 2.8 kg across the entire series-connected PLRCZ assembly (Figure 8). A comparison between the individual load-point testing of series PLRCZ elements (Table 3) and the collective testing of the entire series assembly PLRCZ (Table 4) reveals notable differences in output performance. In Table 3, individual PLRCZ load points were evaluated under 1 kg and 2 kg loads, with the highest output voltage reaching 1 V at load point 10 under the 2 kg condition. In contrast, the entire series-connected PLRCZ system was tested under a higher load of 2.8 kg; the maximum output voltage was only 0.4 V, which is lower than the average voltage measured at individual PLRCZ load points. The reduced voltage output in the series-connected configuration is attributed to the non-uniform distribution of the externally applied 2.8 kg load across the individual PLRCZ elements, resulting in suboptimal mechanical excitation of each sensor.

Figure 8. Overall Testing of the PLRCZ Series Circuit

These findings deviate from the fundamental theory of series circuits, which predicts that the total voltage is equal to the sum of the voltages across individual elements.[21] The results of this study are consistent with the findings reported by Abidin,[22] who demonstrated a significant difference between the output of single piezoelectric sensor elements and those connected in a series configuration. Individual piezoelectric sensors produced higher electrical output, whereas the series-connected configuration exhibited relatively lower performance. This reduction is attributed to the frequent occurrence of discontinuous voltage and current drops in series circuits. Furthermore, piezoelectric sensors based on $BaTiO_3$ material inherently possess very high internal impedance. When arranged in series, the system's total impedance increases substantially, resulting in a severe impedance mismatch with the external load. This mismatch limits efficient power transfer, suppresses current flow, and reduces the effective output voltage at the load.[23] In the present work, no measurable current was detected in the series-connected PLRCZ elements under either 1 kg, 2 kg, or 2.8 kg loading conditions, despite the single-element PLRCZ configuration producing a current of 0.2 mA (Figure 5). This behavior can be attributed to discontinuous current flow within the series circuit, high internal impedance, impedance mismatch with the

external load, as well as mechanical and material-related factors.

As shown in Table 3, the average output voltage per element under a 1 kg load ranged from 0.2 to 0.7 V, while under a 2 kg load it increased to 0.2–1 V. The discrepancies observed in Table 5 arise because when all elements are connected in series, each sensor experiences non-uniform mechanical deformation, preventing ideal voltage accumulation. This effect may be further influenced by the non-uniform distribution of Zn-doped CDs across the sensor surfaces. Elements with a more homogeneous Zn-doped CDs coating exhibit stronger polarization (Figure 9a), whereas elements with sparse or localized coatings show reduced polarization (Figure 9b). Consequently, variations in the distribution of Zn-doped CDs affect dipole polarization and electronic response, resulting in lower overall voltage output in the series-connected PLRCZ configuration.

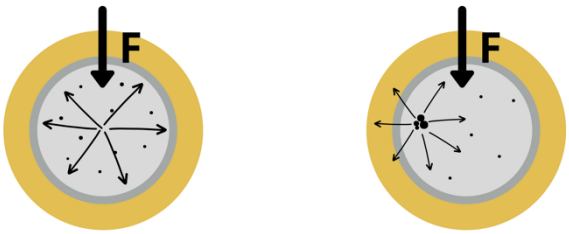

(a) (b)

Figure 9. Distribution of Zn-doped CDs on the Surface of PLRCZ Element, (a) Evenly Distributed, (b) Distributed at a Single Point

Figure 10. Prototype of a CDs-doped Zn layered piezoelectric sensor as a speed bump

Conclusion

This study shows that Zn-doped CDs coatings enhance the mechanical protection and electrical output of BaTiO3-based piezoelectric sensors at the single-element level by improving stress distribution and charge transfer. However, when integrated in a series configuration, the overall energy-harvesting performance decreases due to non-uniform deformation and discontinuous electrical output, leading to low voltage and undetectable current. These findings indicate that, while Zn-doped CDs coatings are effective for improving individual sensor performance, series-connected piezoelectric configurations are not suitable for efficient speedbump energy generation. Future work should focus on alternative circuit configurations, improved coating uniformity, and system-level optimization to enable practical energy-harvesting applications.

Acknowledgment

The author would like to acknowledge the institution for providing the research facilities necessary for this study. The authors also express their sincere gratitude to the supervising lecturers for their valuable guidance and constructive input. Appreciation is further extended to all individuals and parties who provided support and assistance throughout this research.

References

1. Sari RN, Sari YP. Pengaruh Urbanisasi Terhadap Konsumsi Energi di Indonesia. Media Ris Ekon Pembang 2025;2(1):177–84.
2. Purnama R, Susila AR, Febrianti R, Zulfahmi. Pengaruh Subsidi Energi Listrik Mempercepat Transisi Energi Terbarukan. Juremi J Ris Ekon 2024;4(1).
3. Alim MS, Thamrin S, W. Laksmono R. Pemanfaatan Pembangkit Listrik Tenaga Surya sebagai Alternatif Ketahanan Energi Nasional Masa Depan. J Pengabdi Kpd Masy Nusant 2023;4(3):2427–35.
4. Nugraha A, Buchori AS. Investigasi Kemampuan Pembangkit Listrik Tenaga Ombak Laut Mikro Berbasis PVDF. G-Tech J Teknol Terap 2022;6(2):342–9.

5. Fitriani F, Fadillah MS, Christian J. Speedbump Piezoelektrik Sebagai Energi Listrik Alternatif (Studi Kasus Gerbang Kampus UBT). J Elektr Borneo 2023;9(2):60–4.
6. Ghaderiaram A, Schlangen E, Fotouhi M. Analysis of PZT Piezoelectric Sensors in Buckling Mode for Dynamic Strain Measurement. E-J Nondestruct Test [Internet] 2024 [cited 2025 Jun 27];29(7). Available from: https://www.ndt.net/search/docs.php3?id=29596
7. Fu B, Li P, Zhang Y, Wang X, Zheng S, Wang Y. Research on Damage Recognition of Concrete Beams Based on Embedded Piezoelectric Sensors. 2025 [cited 2025 Jun 26];Available from: https://www.ssrn.com/abstract=5165578
8. Muhsinin A, Badruzzaman H, Hendardi AR. Sistem Pemanen Energi Berbasis Piezoelektrik Sebagai Sumber Energi Terbarukan Pada Konstruksi Jalan. Live Appl Sci 2022;2.
9. Sumaiyah, Hasibuan PAz, Tanjung M, Lianto W, Gea S, Piliang A, et al. Hydrothermally nitrogen-doped carbon dots (N-C-dots) from isolated lignin of oil palm empty fruit bunch for bacterial imaging of Staphylococcus aureus. Case Stud Chem Environ Eng 2023;8:100455.
10. Anindita F, Naani L, Permana D, Karelius K, Kedang YI. Study on Utilizing Oil Palm Empty Fruit Bunch Waste into Carbon Nanodots. J Indones Soc Integr Chem 2024;16(2):140–6.
11. Sow AC, Palleau E, Fabre–Francke I, Ratel-Ramond N, Marcelot C, Ressier L. Synthesis of multicolored photoluminescent carbon nanodots and applications to secured tags in anti-counterfeiting, traceability and digital passport product. Carbon Trends 2025;19:100497.
12. Halawa DS, Andhita NA, Pasaribu MH. Carbon Quantum Dots sebagai Sensitiser Sel Surya: Sebuah Tinjauan Sintesis, Mekanisme, dan Aplikasi. Bohr J Cendekia Kim 2025;03(02).
13. Amirsoleimani A, Bahrami Z, Abdoos H, Kafshdouzan K. Synthesis and characterization of Zn-doped carbon dots derived from calendula officinalis and glucose: Antibacterial and photoluminescence properties. Carbon Trends 2025;20:100537.
14. Sidiq A, Syahrillah GRF, Isra M. Studi Experimental Pemanfaatan Speed Bamper (Polisi Tidur) Menjadi Energi Listrik Menggunakan Piezoelektrik. Al-Jazari J Ilm Tek MESIN [Internet] 2021 [cited 2025 Jun 22];6(2). Available from: https://ojs.uniska-bjm.ac.id/index.php/JZR/article/view/6055
15. Apriyanto NP, Firmansyah E, Putranto LM. Piezoelectric Energy Harvester for IoT Sensor Devices. IJITEE Int J Inf Technol Electr Eng 2021;5(4):124.
16. Pradistia RF, Prasetya DA. Pemanfaatan Sensor Piezoelektrik Sebagai Penghasil Sumber Energi Dengan Tekanan Anak Tangga. Emit J Tek Elektro 2022;22(1):55–64.
17. Dona R, Purnamasari N, Wulandari W, Hilmi A, Fauziyah N, Pratapa S. Tensile Strength of PMMA/n-ZrSiO4 Composites Using Dynamic Mechanical Analyzer (DMA). Mater Sci Forum 2021;1028:228–33.
18. Acosta M, Novak N, Rojas V, Patel S, Vaish R, Koruza J, et al. BaTiO3-based piezoelectrics: Fundamentals, current status, and perspectives. Appl Phys Rev 2017;4(4):041305.
19. Tan Y, Zhang J, Wu Y, Wang C, Koval V, Shi B, et al. Unfolding grain size effects in barium titanate ferroelectric ceramics. Sci Rep 2015;5(1):9953.
20. Liu X, Lv S, Fan B, Xing A, Jia B. Ferroelectric Polarization-Enhanced Photocatalysis in BaTiO3-TiO2 Core-Shell Heterostructures. Nanomaterials 2019;9(8):1116.
21. Valemtina MA, Eva Magdalena S, Widodo B. Perancangan Prototype Pembangkit Piezoelektrik Lantai Untuk

Suplai Energi Listrik Lampu Penerangan Pintu Masuk Rumah. J Inform Dan Tek Elektro Terap [Internet] 2025 [cited 2025 Jun 22];13(1). Available from: https://journal.eng.unila.ac.id/index.php/jitet/article/view/5983

22. Abidin Z, Ulul Ilmi, M. Feri Bani Ashari. Desain Speed Bump Penyimpan Energi Berbasis Sensor Piezzoelektrik. J JEETech 2022;3(2):84–9.
23. Rathod VT. A Review of Electric Impedance Matching Techniques for Piezoelectric Sensors, Actuators and Transducers. Electronics 2019;8(2):169.